

# USING DNA ORIGAMI TO EVALUATE MOTOR PROTEIN BINDING PATTERNS

Capstone Manuscript

**Presented By:**

Søren Hough

**ID:** 25595596

**Completion Date:**

March 2014

**Approved By:**

---

Jennifer Ross, PhD, Physics Department

---

John Lopes, PhD, Microbiology Department

---

Wilmore Webley, PhD, Microbiology Department



## ABSTRACT

Title: **Using DNA Origami to Evaluate Motor Protein Binding Patterns**

Author: **Søren Hough**

Thesis/Project Type: **Research Thesis**

Advisor: **Jennifer Ross, Physics Department**

Approved By: **Wilmore Webley, Microbiology Department**

Committee Member: **John Lopes, Microbiology Department**

Cargo is transported around the cell on a complex interconnected matrix of filamentous polymers called microtubules. While studies have been performed on the antagonistic and cooperative behaviors of motor proteins in intracellular transport, it is still unclear how and where motor proteins bind to their cargo. Using DNA origami, a potentially powerful tool for use in transport assays due to the robust and programmable nature of DNA, my project was to create a ~20 nm tetrahedral nanocage to serve as an artificial cargo kinesin-1 intracellular transport. This model system would then be evaluated using single molecule imaging techniques.

## ABSTRACT

Title: **Using DNA Origami to Evaluate Motor Protein Binding Patterns**

Author: **Søren Hough**

Thesis/Project Type: **Research Thesis**

Advisor: **Jennifer Ross, Physics Department**

Approved By: **Wilmore Webley, Microbiology Department**

Committee Member: **John Lopes, Microbiology Department**

Cargo is transported around the cell on a complex interconnected matrix of filamentous polymers called microtubules. While studies have been performed on the antagonistic and cooperative behaviors of motor proteins in intracellular transport, it is still unclear how and where motor proteins bind to their cargo. Using DNA origami, a potentially powerful tool for use in transport assays due to the robust and programmable nature of DNA, my project was to create a ~20 nm tetrahedral nanocage to serve as an artificial cargo kinesin-1 intracellular transport. This model system would then be evaluated using single molecule imaging techniques.



## INTRODUCTION

The cell is the building block of life. It gives an organism its structure and performs essential functions like respiration. Eukaryotic cells rely on a complex network of long filaments called microtubules to keep cells healthy as they complete these fundamental tasks.

Microtubules are proteinaceous filaments which form a widespread matrix throughout the cell. The cell needs these structures to maintain its morphology; without this cytoskeleton, the cell would lose its ability to retain its rigid shape. The role of microtubules extends to everything from the development of neurons to cell differentiation and ciliary beating in key organs in the body (Bailey et al. 2013).

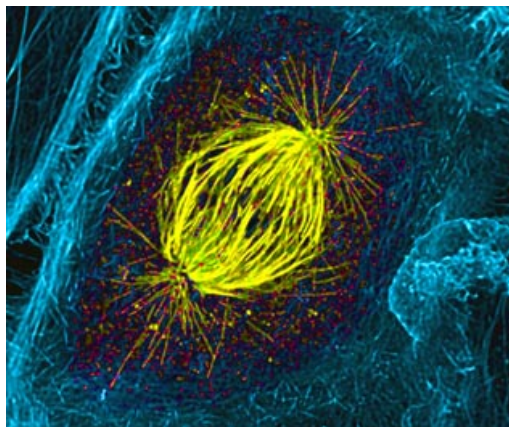


**Figure 1 Mitotic Spindle** – Microtubules are instrumental in cell division. In this image from the Wadsworth Laboratory at UMass Amherst, the mitotic spindle can be seen arranging around chromosomes in the center of the cell. Tubulin has been labeled with anti-tubulin antibodies (yellow) and actin has been labeled with phalloiden (blue).

Microtubules are also essential to the cell cycle. When a cell divides, it duplicates its chromosomes and then cleaves into two daughter cells. This process is highly regulated by microtubules, which first realign themselves in what are called “mitotic spindles,” such that they attach to the kinetochores of duplicated chromosomes (**Fig 1**). During mitosis, the microtubules

pull the chromosomes apart, retreating to opposite poles as the parent cell splits in two (Desai and Mitchison 1997).

The role of microtubules extends beyond the cell cycle, however. One of their most important functions is how they operate together to form an intracellular “highway” system. The cell is crowded. Numerous macromolecules, organelles, and other impediments can prevent essential components from diffusing from one part of the cell to the other without aid. In order to accommodate this limitation, the cell produces a class of macromolecules called motor proteins (Conway et al. 2012).

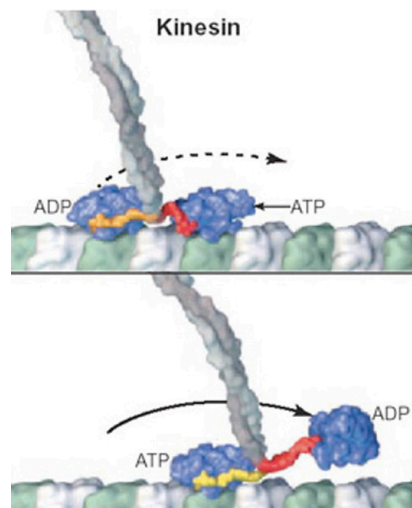


**Figure 2 *Kinesin Motion*** – Kinesin hydrolyzes ATP as it moves hand over hand toward the plus-end of the microtubule (figure adapted from Endres et al. 2006).

There are many types of motor proteins, including the dynein, myosin, and kinesin superfamilies. This study is particularly interested in kinesins, motors specially adapted to microtubules. Using their tail region, they attach to cargo which needs to be moved across the cell. Lower down, their head region binds the microtubule and, with the help of ATP hydrolysis, the whole apparatus “walks” toward its destination - in the case of kinesin, toward the cell wall (**Fig 2**).

This process has been observed using a modern biophysical technique known as single molecule microscopy. More specifically, many research groups have used total internal reflection microscopy, or TIRF, to study cargo transport. TIRF relies on the principle that a high energy input (i.e. a laser) into a small sample will yield visible energy output, albeit at lower levels. Therefore, objects like kinesin and their cargo, which would normally be too small to see with a conventional microscope, become visible when using a high energy laser to visualize them because they, in turn, reflect a low energy output (Ross and Dixit 2010).

Kinesin is a highly processive protein. This means that when it carries cargo, it only makes a short trip along the microtubule before falling off. Once a kinesin lost its spot on the intracellular “highway,” another kinesin will take its place and carry the cargo further. The distance the cargo travels in each increment is known as the “run length.”

In order to increase the run length of kinesin, single molecule microscopy has been used to observe that these proteins have the capacity to work in concert with one another to carry the same cargo (Conway et al. 2012). Conversely, kinesin can operate antagonistically with other motor proteins like dynein, which is known to walk in the opposite direction of kinesin (Derr et al. 2012). However, what is not currently well understood is the manner in which motor proteins arrange themselves on their cargo.

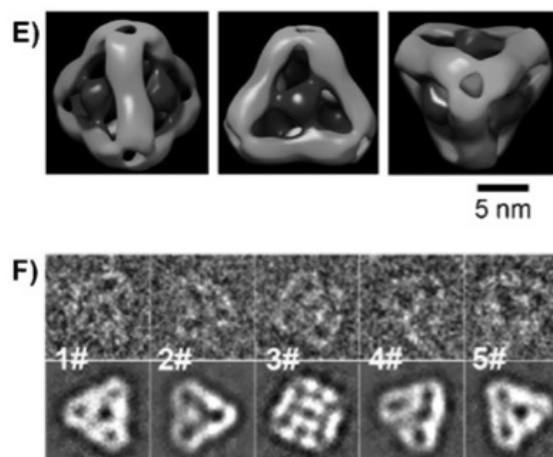


**Figure 3 DNA Tetrahedron** – This diagram shows three different views of a DNA-streptavidin complex created using cryoEM as a template in **E**. **F** shows raw cryoEM images of the structure (top) and 2D projections of those images (bottom) (figure adapted from Zheng et al. 2013).

The field of DNA self-assembly may hold an answer to this question. DNA is notable for being a resilient and programmable tool for molecular manipulation. In a recent study from the Mao Laboratory at Purdue University, it was demonstrated that basic 3D DNA structures could be made using simple base pairing and protein-protein interactions (**Fig. 3**) (Zheng et al. 2013). Using the Mao Lab’s work as a platform, this investigation endeavors to modify a DNA origami structure for use as an artificial cargo for kinesin. The hypothesis is that by controlling where the kinesin molecules bind to the cargo, the effects thereof on measures like run length and run velocity can be determined.

There is precedent for using DNA structures to study intracellular transport. At the Kojima Laboratory at the National Institute of Information and Communications Technology in Japan, it was shown that a SNAP-tag fused motor protein could be bound to DNA through an amino-modifier intermediate. The group used this principle to attach two different kinds of motor proteins (kinesin-1 and Ncd) to one simple 2D DNA structure and then observed the results (Furuta et al. 2013). In a similar experiment, the Reck-Peterson Laboratory attached SNAP-tag-

kinesin and HALO-tag-dynein proteins to a complex DNA scaffold to measure their “tug-of-war” behavior (Derr et al. 2012).

With these principles in mind, this project will involve the tetrahedron structure from the Mao Laboratory and the amino-modifier used by the Kojima Laboratory. The tetrahedron is a 3D structure and therefore offers an advantage when compared with the Kojima DNA structure, but is also less complicated than the Reck-Peterson multi-ringed chassis. Furthermore, the tetrahedron produces a high yield after self-assembly (90%); this means the protocol itself is highly efficient. Finally, starting with the Mao model allows for more complex structures in the future. That group has already created self-assembling DNA octohedra and icosohedra. This means that further studies could use these more advanced origami figures to measure a wider range of kinesin-cargo binding patterns.

Researching both the cytoskeleton and motor proteins is a critical scientific undertaking. Studies have shown that mutations in the molecular transport system can lead to neuronal diseases, birth defects, and cancer. It is therefore key to understand the basic operations of motor proteins, beginning with the kinesin-cargo interface.

## BACKGROUND

### Microtubules

Microtubules are 200 nanometer to 25 micrometer polymeric protein filaments made up of  $\alpha$ - and  $\beta$ -tubulin heterodimers. As they polymerize, they add  $\alpha$  to  $\beta$  in a repeating lattice sequence, eventually curling into a tube that is  $\sim 25$  nanometers in outer diameter and  $\sim 17$  nanometers in inner diameter (Bailey et al. 2013). Each linear row of  $\alpha$  and  $\beta$  is referred to as a protofilament, whereupon motor proteins like kinesin can bind and “walk” as they transport cargo (**Fig. 4**).

The microtubule grows rapidly in length from the plus (+) end, or the end where  $\beta$ -tubulin is exposed. The minus (-) end has exposed  $\alpha$ -tubulin and grows at a slower rate. This results in polarized structures (Pringle et al. 2013). Microtubules arrange so that the minus-end is oriented toward the center of the cell where the microtubule organizing center (MTOC) is found, while the plus-end orients in the direction of the cell membrane where the actin cortex is located (Ross et al. 2008).

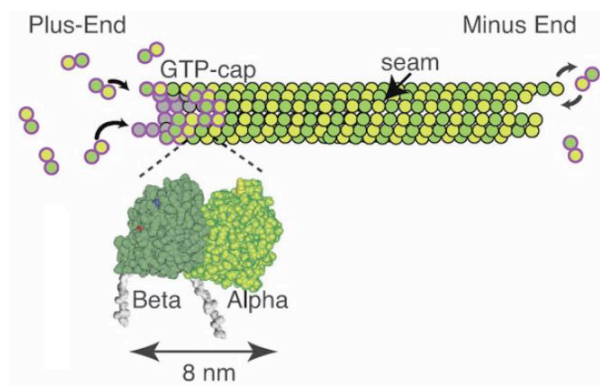


**Figure 4 Microtubule Assembly** – Microtubules are made up of tubulin heterodimers. They are polarized, such that one end has exposed beta tubulin (+) and one has exposed alpha tubulin (-) (figure adapted from Bailey et al. 2013).

Microtubules are mostly rigid, although they do have the capacity to bend to some degree in the presence of stabilizing agents like taxol (Hawkins et al. 2013). They are responsible for several functions in the cell. They give the cell its structure, offering support for the cell to keep its shape. They are also key assets during mitosis as they feature prominently in the cell division process. Finally, they serve as intracellular “highways” along which cargo can be transported by motor proteins.

### Kinesin-1

Kinesin-1 is a processive motor protein homodimer. It is comprised of a coil-coil stalk region, or tail, which binds to cargo, and a head region, which is its motor domain. The head region hydrolyzes ATP to generate energy. Using a hand-over-hand mechanism, the motor “walks” along a single protofilament on the microtubule (**Fig. 5**) (Yildiz et al. 2004). Large cargo, such as organelles or other resources, cannot diffuse easily through the cell on their own. As a supplement, they can be bound to the tail region of kinesin and pulled toward the intracellular region of interest. For the purposes of this project, a truncated but fully functioning kinesin-1 molecule (K560) was used.

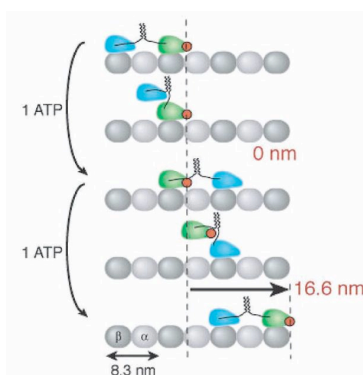


**Figure 5 Kinesin Moves Hand-Over-Hand** – The head region of microtubules moves in a hand over hand fashion along a protofilament “track” on the microtubule (figure adapted from Yildiz et al. 2004).

Kinesin is plus-end directed, distinguishing it from other motor proteins such as dynein. In other words, kinesin brings cargo from the center of the cell toward the periphery while dynein brings cargo in the direction of the nucleus. Once it reaches the actin cortex, the kinesin transfers its cargo to myosin proteins. Myosins then take the cargo to the cell membrane (Ross et al. 2008).

Some studies have been performed on the antagonistic (dynein and kinesin) and cooperative (multiple kinesins) behaviors of motor proteins in intracellular transport (Hendricks et al. 2010; Jolly and Gelfand 2011; Derr et al. 2012). Nevertheless, it is still poorly understood how these motor proteins bind to their cargo.

## DNA Origami

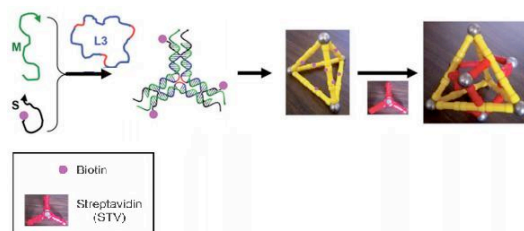


**Figure 6 DNA From Strand to Assembly** – Strands S, M, and L3 will self-assemble into star-shaped DNA nanomotifs. Through base pairing and protein-protein interaction, four of these motifs would then assemble into a DNA tetrahedron (figure adapted from Zhang et al. 2004).

DNA origami is the process by which DNA strands self-assemble into geometric shapes (e.g. tetrahedra, cubes). Due to the highly programmable nature of DNA, these sequences can be modified to change the shape or binding affinity of the resultant structure. This means DNA origami can be used to produce a large variety of structures.



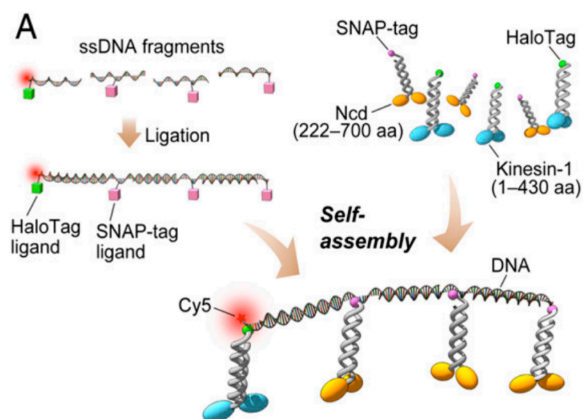


**Figure 7 Attaching Kinesin to DNA** – Here, the Furuta Lab attach SNAP-kinesin and Ncd proteins to self-assembled DNA structures via a ligand intermediate. Not shown in this figure but present in the supplementary information of the Furuta paper are the C6 dT amino-modifiers used as binding locations for the SNAP-tag ligand molecules (figure adapted from Furuta et al. 2012).

The DNA tetrahedron is one of the simplest structures to make using DNA origami. It is formed by biotinylating one of three specific DNA strands and then combining them in a buffer along with streptavidin. Through base pairing and biotin-streptavidin interactions, the origami self-assembles during incubation (**Fig 6**). The sequences must be PAGE-purified before assembly to yield sufficient results (Zhang et al. 2013). The streptavidin used would be Alexa 488, a fluorescent version of the protein which could later be used for tracking the cargo itself in TIRF.

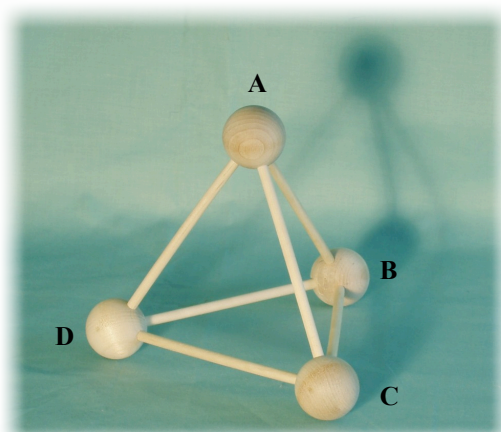


**Figure 8 Model of Tetrahedron** - This diagram indicates the four separate vertices to which the SNAP-kinesin might bind. Each of these vertices contains three “flexible T” sequences regions that allow it to bend into a tetrahedron.

Finally, the sequence would include an amino-modifier from Glen Research to help facilitate attachment to the SNAP-kinesin as described in Furuta et al. 2012 (**Fig. 7**). However, not every L3 strand would include an amino modification. This is because the purpose of this investigation is to establish the effect of binding location on cooperativity between any number of motors (greater than one). In other words, a kinesin might bind to vertices A and B, or vertices A, B, and C, or vertices A, B, C, and D (**Fig. 8**).

### SNAP-tag

SNAP-tag is a New England Biolabs (NEB) proprietary molecule which can be fused with other proteins. For the purposes of this project, it is meant to serve as linker between the motor protein, K560, and the DNA origami. The SNAP-tag will attach to a special ligand from NEB, which in turn will bind to an amino-modified region of the DNA origami (**Fig. 9**) (Furuta et al. 2013).

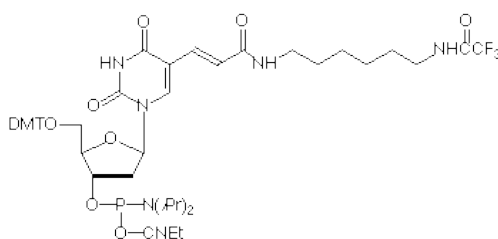


**Figure 9 Amino-Modifier C6 dT from Glen Research** – The molecular structure of the modifier used to link the SNAP-tag ligand to the DNA tetrahedron.

The association of SNAP-tag to the K560 motor protein was requires the use of molecular cloning techniques. By inserting the gene for SNAP-tag into the vector for kinesin, the expressed protein would be a fusion of SNAP-tag and K560. This fusion protein will forthwith be referred to as SNAP-K560.

Note that cloning was first attempted with the Pet-17 Kif1A vector, but was unsuccessful because the Qiagen mini-prep kit contained bad reagents. Although the error was eventually resolved, the Reck-Peterson Lab at Harvard University generously provided a pre-made SNAP-K560 fusion vector to save time. Therefore SNAP-K560 used to transform our bacteria and express the protein, and not SNAP-Kif1A.

In order to track the amount of kinesins attached to a given cargo, a rhodamine fluorophore serve as marker on every strand that was amino-modified. Therefore, during analysis, the presence of rhodamine would also indicate that the cargo in question included an amino-modified sequence. Taking this logic further, higher intensity of rhodamine fluoresce would indicate how many amino-modified sequences there are in that cargo, and therefore how many kinesin molecules are attached.

### **Photobleaching**

Photobleaching is a phenomenon wherein a fluorophore is excited with enough light that it loses its fluorescence. This process can be used to evaluate the number of fluorophores in a given location by recording fluorescence intensity as each fluorophore photobleaches (or “goes out”). In this study, rhodamine would be added to the DNA origami every time the amino-modifier was present. When looking at the molecule using TIRF microscopy, intensity and photobleaching data would indicate how many rhodamine molecules, and therefore how many SNAP-K560 proteins, were attached. In order to better understand the photobleaching process before the actual assessment of the modified DNA origami structures, photobleaching assays were performed using GFP.

## MATERIALS AND METHODS

### Stock Buffers

Stock buffers and reagents were created, including 1M Tris pH 8.0, 1M IPTG, ampicillin at 100 mg/mL, and DNA loading dye. Deoxy was created using glucose, catalase, and ddH<sub>2</sub>O. Lysogeny broth (LB) was created using tryptone, yeast extract, NaCl, and ddH<sub>2</sub>O. EDTA was made using disodium EDTA•2H<sub>2</sub>O and ddH<sub>2</sub>O. DNA loading dye is created using glycerol, 10% SDS, .5 M EDTA, and bromophenol blue.

### Photobleaching

For the photobleaching assay, a chamber was created by rinsing a microscope slide and cover slide with ddH<sub>2</sub>O and then 70% ethanol. Once dry, double sided tape was placed such that it created a thin channel on the slide about 3 mm wide. The channel held about 10 microliters. A cover slip was placed over the tape and channel, creating a chamber. The butt of a marker was used to seal the chamber.

Then, 1%  $\alpha$ -GFP was flowed in and the chamber was incubated at room temperature for 5 minutes. Afterward, 1:500 GFP was flowed into the chamber. The chamber was subsequently imaged using TIRF. By analyzing the TIRF capture using ImageJ, the fluorescence data was graphed.

### **Polymerase Chain Reaction (PCR)**

To run a PCR, dNTP was mixed with a vector plasmid, a forward primer, a reverse primer, 5X HF buffer, DMSO, ddH<sub>2</sub>O, and Phusion enzyme in several different PCR tubes. Based on melting and annealing data, the tubes were then run in a PCR machine at varying temperatures to determine which condition yielded the most product. PCR cycles were set to run at 98°C for 1 minute, (35 cycles of 98°C for 10 seconds, the varying temperature for 20 seconds, 72°C for 1 minute), 72°C for 5 minutes, with a final resting temperature of 4°C. The PCR product was then purified using the PCR purification kit.

### **Restriction Enzyme Digest**

To run a KpnI digestion, Kif1A vector was mixed with 10X NEB Buffer 2, 100X NEB BSA, and KpnI. The PCR product was mixed with NEB Buffer 1, 100X BSA, ddH<sub>2</sub>O, and KpnI. in a separate 1.5 mL tube. The tubes were then incubated at 37°C for 1 hour. Next, the digests were spiked with KpnI and incubated for another hour. The Kif1A digest was subsequently treated with CIP and incubated at 37°C for one hour. Finally, Kif1A and the PCR product were both purified post-digestion using the Qiagen PCR purification kit.

### **DNA Ligation**

The 3:1 and 6:1 ligation volumes for the Kif1A vector and PCR insert were determined by multiplying 3 or 6 (respectively) by the insert length over the vector length, and then by the vector mass. Three different ligations were then set up. For the 3:1 and 6:1 ligations, the calculated volumes of Kif1A and SNAP were mixed with 2X Quick Ligase Buffer, Quick Ligase,

and ddH<sub>2</sub>O. The third “ligation” was set up as a control with just Kif1A, 2X Quick Ligase Buffer, and Quick Ligase. All three ligations were run for 10 minutes at room temperature.

### **1% Agarose DNA Gel**

To prepare a 1% agarose gel, agarose was added to 1X TAE buffer. This was then microwaved and shaken until the solution was thoroughly mixed. Ethidium bromide was added to the agarose mixture and poured into a gel castor. A comb was added to provide wells for adding the DNA samples. After adding the samples, the gel was then run and subsequently examined under UV light.

### **Chemically Competent *E. coli* Cells (Rosetta and DH5 $\alpha$ )**

To create competent *E. coli* cells, stock cells were first streaked on an lysogeny broth (LB) agar plate and grown at 37°C overnight. In the case of Rosetta cells, the plate contained chloramphenicol. On the DH5 $\alpha$  plate, no chloramphenicol was added. The following day, a colony from each plate was added to two separate tubes of liquid LB to create starter cultures. Again, the Rosetta LB contained chloramphenicol while the DH5 $\alpha$  LB did not. The LB tubes were placed into an incubator and shaken overnight.

The starter cultures were added to larger flasks of LB (one with chloramphenicol for Rosetta, the other without for DH5 $\alpha$ ). The cells were grown to an OD<sub>600</sub> of .4. They were then poured into centrifuge tubes and incubated on ice for 20 minutes. The tubes were spun at 3,000 x g for at 4°C for 10 minutes.

The media was then poured off, the pellet resuspended in .1 M CaCl<sub>2</sub>, and the suspension incubated on ice for 40 minutes. After, the resuspended cells were centrifuged at 3,000 x g at 4°C for 10 minutes. In the final step, the supernatant was poured off and the pellet resuspended in .1 M CaCl<sub>2</sub> + 15% glycerol. The cells were aliquoted, drop frozen, and stored at -80°C.

### **Bacterial Transformation**

To transform bacteria for subsequent protein purification, a tube of competent Rosetta cells was thawed on ice. The DNA vector (using an ampicillin antibiotic marker) was then added. Afterward, the tube was incubated for 30 minutes, heat shocked at 45 seconds at 42°C, and incubated on ice again for another 2 minutes. LB was added to the tube and then the tube was incubated for 1 hour at 37°C. Finally, the cells were plated on ampicillin-treated LB agar and incubated overnight at 37°C.

### **Protein Purification**

A flask of liquid TPM media was first created using tryptone, yeast extract, NaCl, Na<sub>2</sub>HPO<sub>4</sub>, and KH<sub>2</sub>PO<sub>4</sub>, along with a solution of 20% glucose. A starter culture using a transformed Rosetta cell colony, TPM media, 20% glucose, and ampicillin was incubated overnight at 37°C in the shaker. The next day, the starter culture was added to the TPM flask and grown to an OD<sub>600</sub> of 1.6. Once the broth was at the correct optical density, the flask was induced with IPTG and shaken overnight at room temperature.

The next day, the cells were placed in centrifuge bottles and spun at 5,000 RPM at 4°C for ten minutes. The supernatant was then poured off before the pellet was moved into a separate

conical and frozen at  $-80^{\circ}\text{C}$  for 60 minutes. Lysis buffer was created using 2 mg/mL aprotonin, 2 mg/mL leupeptin, 2 mg/mL pepstatin, tween-20, and 100 mM ATP. After freezing, the pellets were resuspended in the lysis buffer. Lysozyme and DnaseI were also added. The conical was then rocked at  $4^{\circ}\text{C}$  for 20 minutes, sonicated for 1 minute on ice, and centrifuged again at 40,000 x g at  $4^{\circ}\text{C}$  for 30 minutes.

The supernatant from the centrifuged tube was subsequently mixed with equilibrated nickel (Ni) beads and 1M imidazole before getting rocked at  $4^{\circ}\text{C}$  for 1 hour. The supernatant and beads mix was then run through a column. Afterwards, wash and elution buffer were used to fractionate the sample out. A dot blot test was done to confirm which elution(s) contained protein.

The elution was then buffer exchanged. To do this, an NAP 5 column was drained and PEM100 and 100 mM ATP was added to the column gel bed. The sample was then added to the column and allowed to move through the gel bed into collection a tube. The sample was finally mixed with sucrose, aliquotted, and drop frozen for storage at  $-80^{\circ}\text{C}$ .

A small sample was taken at each major phase of this procedure. These samples were used later for protein gel verification. Following purification, Leslie Conway ran a BSA standards gel to check the concentration of the protein.

### **8% Polyacrylamide Protein Gel**

To make a protein gel, the glass holding plates were first cleaned with ethanol. Then, the plates were put into the gel holder apparatus. Resolving buffer and stacking buffer were both prepared. Resolving and stacking buffer contained ddH<sub>2</sub>O, 30% acrylamide, stock resolving



buffer, 10% SDS, APS, and TEMED, each at varying concentrations depending on the buffer in question. APS and TEMED were not added until the moment of pouring, as they were the solidifying agents in the solution. All ingredients were kept on ice until needed.

Resolving buffer was poured in between the cleaned ethanol plates. Stacking was added on top of the resolving buffer. A comb was then placed in the gel, creating wells. After the gel had solidified, the samples were added and the gel was run at a set voltage. Once complete, the gel was analyzed to make sure that the protein in question had been purified based on band density and run distance on the gel.

### Gliding Assay

To perform a gliding assay, stock solutions were made. Microtubules infused with fluorescent Dylite-550 were diluted 1:100 in 2 mM taxol and PEM-100. Chamber wash was made using PEM-100, 10 mg/mL BSA, 2 mM taxol, and 1M DTT. Motility mix was made using PEM-100, 2 mM taxol, 1M DTT, and .1 M ATP. A flow chamber was created using the same process outlined in the photobleaching protocol.

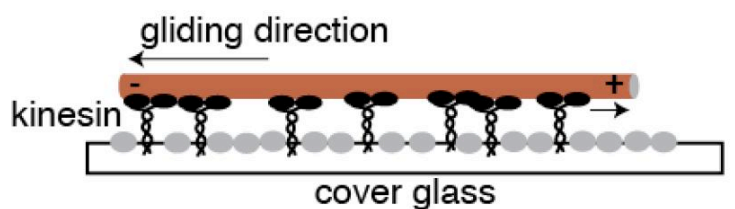


**Figure 10 Gliding Assay** – Kinesin molecules adhere to the cover glass such that their tail region is pointed down and their head region is pointed up. When microtubules are flowed onto the kinesin molecules, the motor proteins pull them along. Viewed with the optical trap, the microtubules can be seen gliding over the kinesin (figure adapted from Pringle et al. 2013).

To run the assay, the motor protein K560 was flowed into the chamber. The chamber was incubated for five minutes. Then, the chamber wash was added, and a Kimwipe was used to wick

from the opposite side. Afterwards, the 1:100 microtubule mix was flowed in, again wicking from the opposite side. The chamber was incubated at room temperature for another five minutes. Finally, glucose and deoxy were added to the motility mix, which was itself added as the chamber was wicked once more. The chamber was then ready for observation in the optical trap.

### **Molecular Motility Experiment**

For a molecular motility assay, a mix of 2%  $\alpha$ -tubulin using PEM-20 and  $\alpha$ -tubulin was created. Then, a .5% mix of pluronic F127 was made using PEM-20 and 5% pluronic F127. Next, a wash buffer was made using PEM-20, 2 mM taxol, and 1 M DTT. Afterward, a 1:50 GFP-kinesin dilution was made using PEM-20, GFP-kinesin and DTT. These were all kept on ice. Finally, a 1:100 microtubule dilution was created using PEM-20 and microtubule stock. This was not kept on ice.

A flow chamber was created using a clean slide, double sided tape, and a cover slip. The 2%  $\alpha$ -tubulin mix was flowed in and the chamber was incubated at room temperature for five minutes. Then, the .5% pluronic F127 mix was added and again the chamber was incubated for five minutes. Subsequently, the 1:100 microtubule mix was added and the chamber was incubated at room temperature for 10 minutes.

While the chamber was incubating, a motility mix was created using PEM-20, 5% pluronic F127, 2 mM taxol, 10 mg/mL BSA, 1M DTT, 300 mg/mL glucose, deoxy, 1:50 GFP-kinesin, and .1 M ATP. The ATP was only added just before the mix was flowed into the

chamber. The wash buffer was then added to the chamber, followed by the motility mix. The chamber was then brought to the 3D super resolution microscope.

### **DNA Tetrahedron Assembly** (*Assay Not Completed*)

For tetrahedron assembly, a TAE/Mg<sup>2+</sup> buffer would be added to a 1.5 mL tube. Then, the L3 strand at 75 nM, the M strand at 225 nM, and the biotinylated S strand at 225 nM would be added to the buffer and mixed. The tubes would then be floated in a beaker, creating a 95°C water bath.

That beaker would then be covered with aluminum foil and placed in a styrofoam insulating box. The box would then be covered and allowed to cool at room temperature for 48 hours. Finally, the tetrahedron would be verified in both an agarose gel to check the DNA structure and on a 4% native PAGE to verify the protein components of the origami.

## RESULTS

### DNA Origami Paper Template

Using sequence data from the Mao Laboratory at Purdue University, a detailed paper model of the final DNA tetrahedron was created in order to visualize the cargo. This paper model was assembled out of four separate nanomotifs which, when connected at their overhanging M- (green) and S-strand (black) ends, yielded a complete tetrahedron (**Fig. 11**).

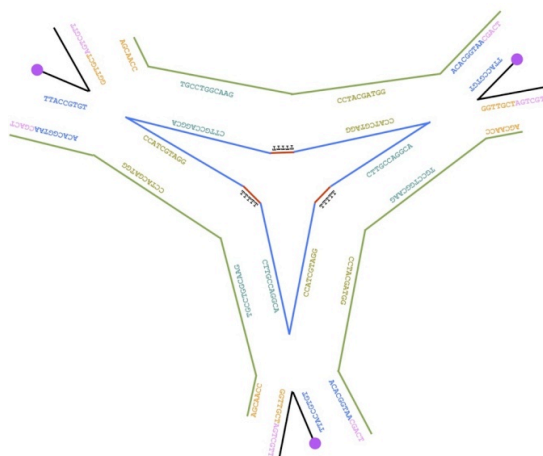


**Figure 11 DNA Nanomotif Diagram** – The full sequence of the S (black), M (green), and L3 (blue) strands used to create the DNA tetrahedron. Purple represents the biotin while the red represents a flexible T-region (a vertex of the completed structure).

In this diagram, the red sequence in the L3 strand (blue) represents the “flexible T-region.” This region constitutes one the four vertices in the completed tetrahedron. Also, because this region is not important for base pairing, it is the region where several DNA modifications would take place: namely, the C6 dT amino-modifier and rhodamine fluorophore. The purple circles represent the biotinylation of the S-strands.

## Cloning and Ligation to Create SNAP-Kif1A

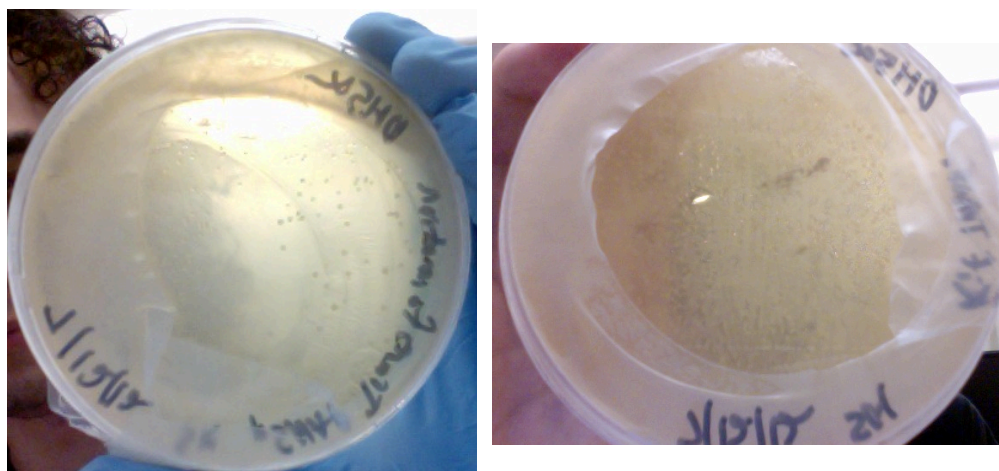


**Figure 13 *DH5α Transformations*** – DH5 $\alpha$  cells transformed with pSNAP (left) and Kif1A vector (right) on LB plate.

The first step in producing SNAP-kinesin was to transform both the Kif1A and pSNAP vectors into DH5 $\alpha$  cells (**Fig. 13**). Then, the DNA was extracted from the transformed colonies. A PCR was subsequently performed on the pSNAP DNA to yield a high quantity of SNAP-tag genes (**Fig 14**). This gene was then cloned into the Kif1A vector via digestion and ligation.

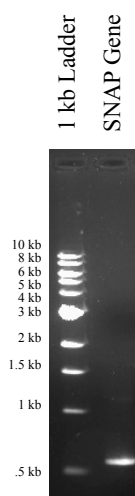


**Figure 14 *SNAP PCR*** – This agarose gel shows the SNAP-tag gene amplified from the pSNAP vector.

After transforming new DH5 $\alpha$  cells with 6:1 and 3:1 ligated DNA, a mini-prep was performed to confirm the ligated vectors contained the SNAP gene. These vectors were then treated with KpnI and run on a gel (**Fig. 15**). Unfortunately, none of the bands showed a second, smaller SNAP sequence, indicating that the ligation did not work.

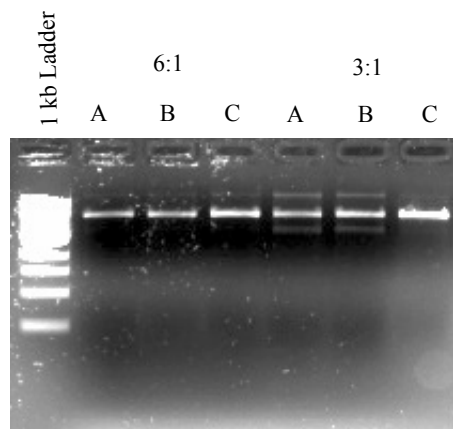


**Figure 15 DNA Ligation Check** – DNA purified from colonies transformed with 6:1 and 3:1 ligated vectors were digested with KpnI and yielded no second band (the SNAP insert). Lanes A and B in the 3:1 ligation show an incomplete digestion with KpnI.

After troubleshooting, it was decided that the Kif1A vector was not at a higher concentration prior to ligation. To fix this, three different Kif1A samples were treated with both KpnI and CIP (**Fig. 16A**). They were then mixed together through gel purification using a second Qiagen kit and run on a gel to determine the concentration (**Fig. 16B**). This still yielded a relatively low  $\sim 20$  ng/ $\mu$ L.

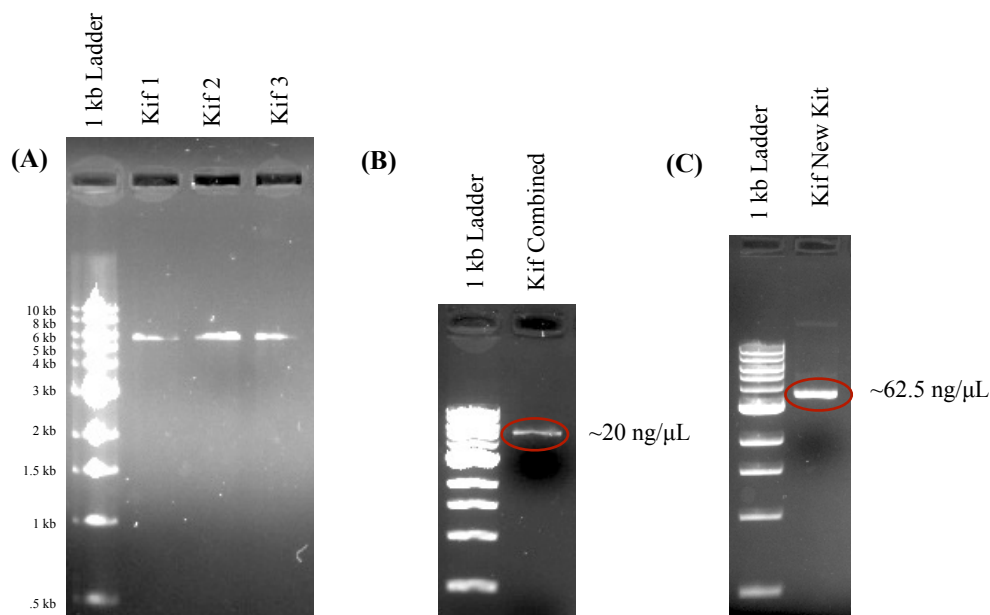


**Figure 16 (A) Three Kif1A Samples** – This gel shows three different Kif1A samples treated with both KpnI and CIP. **(B) Kif1A Sample Concentration** – A concentration check of the gel-purified combination of the samples from (A). **(C) Kif1A New Kit** – Using a new Qiagen kit, the Kif1A vector was again digested and treated with CIP, yielding a higher concentration.

After determining that the Qiagen kit may have faulty reagents, a new Qiagen kit was purchased. A new sample of Kif1A was purified, digested with KpnI, and treated with CIP. Then, the sample was run on a DNA gel. The result showed a marked improvement in concentration, yielding  $\sim 62.5$  ng/ $\mu$ L (**Fig 16C**).

## Protein Purification

Due to time constraints, the SNAP-Kif1A cloning assays were set aside after a SNAP-K560 vector arrived from the Reck-Peterson lab. This vector transformed into bacteria which were then grown in culture. The protein was purified using affinity column chromatography. The protein was then run on a polyacrylamide gel (**Fig 17**).

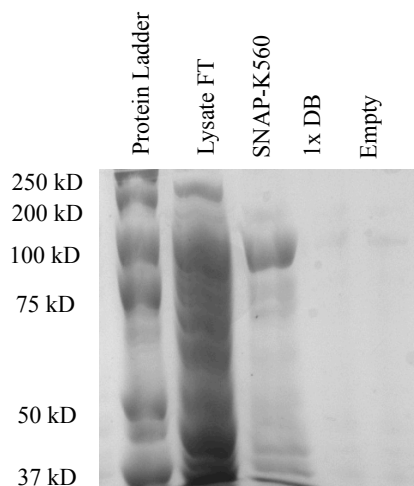


**Figure 17 Kinesin Protein Gel** – This gel shows the purified SNAP-K560 alongside the unpurified lysate flow-through (FT). The 1X DB lane indicates a control containing loading buffer and no protein.

Leslie Conway, a post-doctoral researcher in the laboratory, determined the concentration of the SNAP-K560 purification using BSA standards. She ran four separate BSA samples on a polyacrylamide gel and compared them to the purified SNAP-K560 protein. The result of this test showed that the concentration of SNAP-K560 was 672 nM (**Fig. 18**).

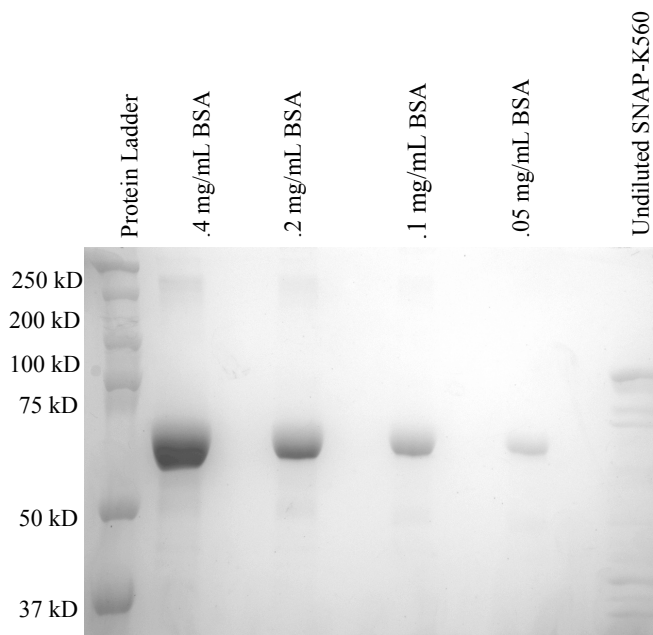


**Figure 18 BSA Standards Gel** – This protein gel from Leslie Conway shows a BSA standard used to establish the concentration of the purified SNAP-K560. Using this method, the protein was determined to be 672 nM.



## Gliding Assay

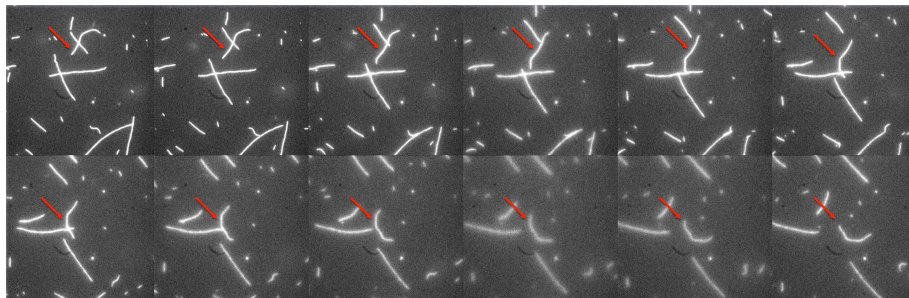


**Figure 19 SNAP-K560 Gliding Assay** – This time lapse shows 12 frames taken ~9 seconds apart with the optical trap. The microtubules were tagged with a Dylight 550 fluorophore. The red arrow is a reference point to indicate one particular microtubule as it glides over the unlabeled SNAP-K560.

To test the functionality of the purified SNAP-kinesin, a gliding assay was performed.

The time lapse in **Fig. 19** shows that the microtubules did move inside the flow chamber. This indicates that the kinesin motors were functional because they pulled the fluorescently labeled microtubules on top of them as described in the diagram in **Fig. 10**.

## Molecular Motility Assay

After capturing GFP-kinesin run lengths using a super resolution microscope, the data was then analyzed for run length and velocity. For each motor, the GFP-kinesin was measured using ImageJ to determine the run length. To calculate this value the distance traveled in pixels was multiplied by the conversion ratio of microns to pixels (.044 microns/pixel). This conversion ratio was determined by dividing the CCD native magnification (16 microns/pixel) by the 60X objective, then by the 1.5X tube lens, and finally by the 4X beam expander.

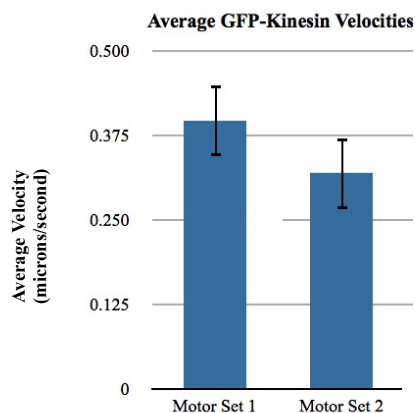


**Figure 20 Motor Velocities** – This graph shows the average velocity of two sets of motors. The first set (n=6) captured by Michael Gramlich, a post-doc in the lab. The second set (n=7) was captured by this author.

After multiplying the conversion ratio (.044 microns/pixel) by the run length (in pixels), this value (in microns) was used to find the velocity. To establish how much time had passed during the run, each frame displaying the run was counted and then multiplied the exposure time (500 milliseconds). This yielded the runtime in seconds. Finally, dividing the run distance (in microns) by the runtime (in seconds) yielded run velocity (microns/second) (**Fig. 20**).

### **GFP Photobleaching Analysis**

After running the photobleaching assay using TIRF, several different analytical parameters were tested. First, the background subtraction feature in ImageJ was evaluated to see if it created a clearer step size between the fluorescing and non-fluorescing GFP protein. Second, the size of the capture area was expanded from 7x7 pixels to 14x14 pixels. These parameters were then changed in concert. The data did not indicate any significant change between these four conditions (**Fig. 12**).

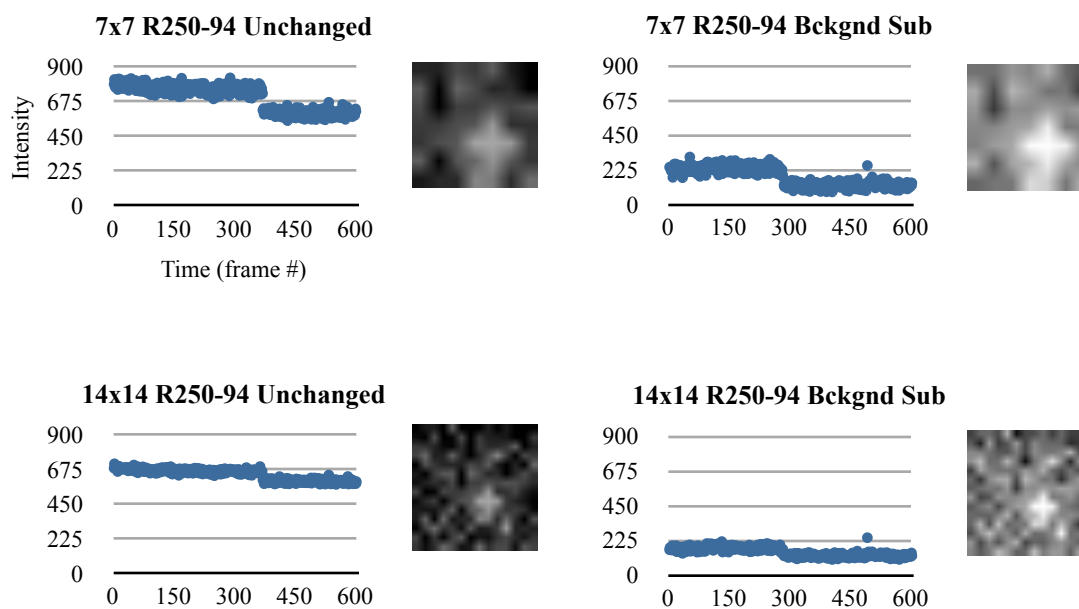


**Figure 12 Analysis of One GFP ROI** – This data shows the parameter changes used to analyze GFP photobleaching: region size and background subtraction. The ROI (region of interest) shown is R250-94.

There were no second steps in any of the analyzed GFP samples. Despite the probability of locating a dimerized GFP molecule in this assay, none of the data suggests that a two-step photobleaching took place. All GFP data resembled the one-step pattern exhibited by ROI (region of interest) R250-94 in **Fig. 12**.

## DISCUSSION

The first step in this investigation was to design and visualize the 3D DNA nanocage origami outline in Zheng et al. 2013. To do this, a paper model was created which allowed a magnified look at one of the four nanomotifs which would anneal to one another to create a tetrahedron during self-assembly. By using this large model, it was decided that the optimal place to modify the DNA with the rhodamine fluorophore and amino-modifier was the flexible T-region at the vertices. This area was picked because it is not involved in base pairing in the final structure and therefore appeared to be the least structurally integral region.

Following the conceptual design of the cargo was the creation of the molecular motors that would carry it. This was achieved through molecular cloning assays. After running a successful PCR of the SNAP gene from the pSNAP vector, the next phase involved inserting that gene into a digested Kif1A vector. However, it turned out that the Kif1A vector did not include sufficient endonuclease cleavage sites where the SNAP gene was to be added. Therefore, it was decided to use one endonuclease, KpnI, and then treat the resultant sticky ends with alkaline phosphatase (CIP) to prevent accidental re-ligation of the vector.

After several attempts at digestion, CIP treatment, and ligation with the SNAP gene, it was determined that the problem may be the relatively low concentrations of Kif1A vector extracted from transformed DH5 $\alpha$ . Therefore, the Kif1A was concentrated by gel purifying three separate samples of the vector. Again, the resulting concentrating was low ( $\sim 20$  ng/ $\mu$ L).

Finally, after several attempts at troubleshooting, it was hypothesized that the mini-prep kit from Qiagen contained faulty reagents. After purchasing new equipment, the subsequent

mini-prep showed more than a three-fold increase in Kif1A concentration (~62.5 ng/ $\mu$ L).

However, despite achieving a higher concentration of Kif1A, at this point in the investigation the Reck-Peterson Lab was able to provide a SNAP-K560 fusion protein vector. This vector was purified using affinity column chromatography

Following the purification, the SNAP-K560 was tested with a gliding assay. The timelapse results in **Fig. 19** clearly show microtubules twisting and turning as they glide in and out of the field of view. This is indicative of functional kinesin, bound to the glass slide while pulling the unbound microtubules up above them. The microtubules were made with Dylite 550 so that they could be observed fluorescently, while the SNAP-K560 were not.

With the fusion protein made and functional, the next step was to prepare for the molecular motility assay. In this experiment, fluorescently labeled motor proteins were mixed with ATP and other reagents before being examined using TIRF microscopy. Then, using image capture software, video of the motility was taken and then analyzed through ImageJ. This process was a model for the analysis of SNAP-K560 as it carried rhodamine-tagged DNA cargo.

In another preparatory exercise, GFP was visualized using TIRF to establish a protocol for photobleaching analysis. This process was meant to mimic the photobleaching analysis that would be done on the rhodamine cargo in the final experiments. By graphing the intensity of numerous GFP molecules as they fluoresced and then went out, a step-like trend was observed. However, none of the data suggested that any of the GFP molecules had dimerized; this would have required a two-step trend. Therefore, it remains unclear whether it would be possible to determine the amount of rhodamines bound to a single cargo.

## CONCLUSION

After designing the oligo modifications based on the designs from the Mao and Kojima Labs, the order was sent to a private DNA synthesis company. Unfortunately, the company was unable to produce the oligos needed after attempting five rounds of synthesis. Therefore, the DNA self-assembly protocol was never attempted.

Had the sequences come in, the next phase of the experiment would have been to work through this protocol to create modified DNA tetrahedra. Then, these tetrahedra would have been analyzed using total internal reflection fluorescence (TIRF) to measure run length and run velocity as it corresponds to kinesin arrangement on the artificial cargo. To determine the kinesins attached to the cargo, the rhodamine molecules on the cargo would have been analyzed using the photobleaching technique.

Although this project did not reach completion, its fundamental ideas show immense promise. Self-assembling complex DNA origami has already been shown to work as a tool in motor protein assays (Derr et al. 2012; Furuta et al. 2013). Given that these modified sequences were too difficult to synthesize, perhaps it is better to return to the planning stages and redesign the oligos with simplicity and an alternative approach in mind.

Cargo transport by kinesin is in many ways still a mystery. Nevertheless, advances in single molecule microscopy (e.g. TIRF, STORM, PALM) have helped the field forward immensely. These tools have helped reveal the answers to fundamental questions about the process, and hopefully, with the help of tools like DNA origami, they will continue to illuminate

the inner workings of the cell in years to come. Ultimately, this will lead to a strong interface between the worlds of molecular biophysics and medical therapeutics.

## ACKNOWLEDGEMENTS

I had the good fortune to work with an incredibly supportive group of scientists, professors, and advisors who helped me finish this manuscript. Notably, Leslie Conway, PhD, was an outstanding mentor to me throughout this endeavor. As noted in the manuscript, she helped directly by working on various assays that were complementary to my project. Of course my advisor, Jennifer Ross, PhD, was remarkable as she donated her patience and good will to my success. I could not list the ways in which she has helped me become a better scientist, but I know that I would not be where I am today without her.

Daniel Diaz, PhD, was a postdoctoral researcher whose expertise helped immensely with the molecular portion of my assays. Megan Bailey is a graduate student who always offered her assistance with TIRF and the optical trap despite her busy schedule. Undergraduates Amanda Tan and Kasmira “Taki” Stanhope both created a wonderful work environment for me and helped me complete administrative tasks around the lab. I would also like to thank the Reck-Peterson Lab at Harvard for providing us with the SNAP-kinesin vector and the Mao Lab at Purdue for their helpful advice concerning DNA origami.

I would be remiss if I did not thank John Lopes, PhD, without whom I might not have pursued the departmental honors track through the Commonwealth Honors College. In the same vein, thank you to Yehudit Heller, PhD, whose CHC guidance helped me complete all of the requisites necessary for this program. Finally, thank you to Wilmore Webley, PhD, who has been an invaluable mentor, professor, advisor, and friend during my time in the microbiology undergraduate program at the University of Massachusetts.



## Bibliography

- Bailey M, Conway L, Gramlich MW, Hawkins TL, Ross JL. *Modern methods to interrogate microtubule dynamics*. Integr Biol (Camb). 2013 Nov;5(11):1324-33. doi: 10.1039/c3ib40124c. Epub 2013 Sep 24. PubMed PMID: 24061278.
- Conway L, Wood D, Tüzel E, Ross JL. *Motor transport of self-assembled cargos in crowded environments*. Proc Natl Acad Sci U S A. 2012 Dec 18;109(51):20814-9. doi: 10.1073/pnas.1209304109. Epub 2012 Dec 3. PubMed PMID: 23213204; PubMed Central PMCID: PMC3529018.
- Derr ND, Goodman BS, Jungmann R, Leschziner AE, Shih WM, Reck-Peterson SL. *Tug-of-war in motor protein ensembles revealed with a programmable DNA origami scaffold*. Science. 2012 Nov 2;338(6107):662-5. doi: 10.1126/science.1226734. Epub 2012 Oct 11. PubMed PMID: 23065903.
- Desai A, Mitchison TJ. *Microtubule polymerization dynamics*. Annu Rev Cell Dev Biol. 1997;13:83-117. Review. PubMed PMID: 9442869.
- Endres NF, Yoshioka C, Milligan RA, Vale RD. *A lever-arm rotation drives motility of the minus-end-directed kinesin Ncd*. Nature. 2006 Feb 16;439(7078):875-8. Epub 2005 Dec 28. PubMed PMID: 16382238; PubMed Central PMCID: PMC2851630.
- Furuta K, Furuta A, Toyoshima YY, Amino M, Oiwa K, Kojima H. *Measuring collective transport by defined numbers of processive and nonprocessive kinesin motors*. Proc Natl Acad Sci USA. 2013 Jan 8;110(2):501-6. doi: 10.1073/pnas.1201390110. Epub 2012 Dec 24. PubMed PMID: 23267076; PubMed Central PMCID: PMC3545764.
- Hawkins TL, Sept D, Mogessie B, Straube A, Ross JL. *Mechanical properties of doubly stabilized microtubule filaments*. Biophys J. 2013 Apr 2;104(7):1517-28. doi: 10.1016/j.bpj.2013.02.026. PubMed PMID: 23561528; PubMed Central PMCID: PMC3617445.
- Hendricks AG, Perlson E, Ross JL, Schroeder HW 3rd, Tokito M, Holzbaur EL. *Motor coordination via a tug-of-war mechanism drives bidirectional vesicle transport*. Curr Biol. 2010 Apr 27;20(8):697-702. doi: 10.1016/j.cub.2010.02.058. Epub 2010 Apr 15. PubMed PMID: 20399099; PubMed Central PMCID: PMC2908734.
- Jolly AL, Gelfand VI. *Bidirectional intracellular transport: utility and mechanism*. Biochem Soc Trans. 2011 Oct;39(5):1126-30. doi: 10.1042/BST0391126. PubMed PMID: 21936776; PubMed Central PMCID: PMC3410738.

Pringle J, Muthukumar A, Tan A, Crankshaw L, Conway L, Ross JL. *Microtubule organization by kinesin motors and microtubule crosslinking protein MAP65*. J Phys Condens Matter. 2013 Sep 18;25(37):374103. doi: 10.1088/0953-8984/25/37/374103. Epub 2013 Aug 15. PubMed PMID: 23945219.

Ross JL, Dixit R. *Multiple color single molecule TIRF imaging and tracking of MAPs and motors*. Methods Cell Biol. 2010;95:521-42. doi: 10.1016/S0091-679X(10)95026-7. Review. PubMed PMID: 20466151.

Yildiz A, Tomishige M, Vale RD, Selvin PR. *Kinesin walks hand-over-hand*. Science. 2004 Jan 30;303(5658):676-8. Epub 2003 Dec 18. PubMed PMID: 14684828.

Zhang C, Tian C, Guo F, Liu Z, Jiang W, Mao C. *DNA-directed three-dimensional protein organization*. Angew Chem Int Ed Engl. 2012 Apr 2;51(14):3382-5. doi: 10.1002/anie.201108710. Epub 2012 Feb 28. PubMed PMID: 22374892.